Scanning ARM Cloud Radars. Part I: Operational Sampling Strategies

PAVLOS KOLLIAS

Department of Atmospheric and Oceanic Sciences, McGill University, Montreal, Quebec, Canada

NITIN BHARADWAJ AND KEVIN WIDENER

Pacific Northwest National Laboratory, Richland, Washington

IENG JO

Department of Atmospheric and Oceanic Sciences, McGill University, Montreal, Quebec, Canada

KAREN JOHNSON

Brookhaven National Laboratory, Upton, New York

(Manuscript received 12 February 2013, in final form 3 December 2013)

ABSTRACT

The acquisition of scanning cloud radars by the Atmospheric Radiation Measurement (ARM) program and research institutions around the world generates the need for developing operational scan strategies for cloud radars. Here, the first generation of sampling strategies for the scanning ARM cloud radars (SACRs) is presented. These scan strategies are designed to address the scientific objectives of ARM; however, they introduce an initial framework for operational scanning cloud radars. While the weather community uses scan strategies that are based on a sequence of scans at constant elevations, the SACR scan strategies are based on a sequence of scans at constant azimuth. This is attributed to the cloud geometrical properties, which are vastly different from the rain and snow shafts that are the primary targets of precipitation radars; the need to cover the cone of silence; and the scanning limitations of the SACRs. A ''cloud surveillance'' scan strategy is introduced that is based on a sequence of horizon-to-horizon range–height indicator (RHI) scans that sample the hemispherical sky (HS) every 30° azimuth (HSRHI). The HSRHI scan strategy is complimented with a low-elevation plan position indicator (PPI) scan. The HSRHI and PPI are repeated every 30 min to provide a static view of the cloud conditions around the SACR location. Between the HSRHI and PPI scan strategies, other scan strategies are introduced depending on the cloud conditions. In the future, information about the atmospheric cloud state will be used in a closed-loop process to optimize the selection of the SACR scan strategy.

1. Introduction

The U.S. Department of Energy (DOE) Atmospheric Radiation Measurement (ARM) program has been in the forefront of climate research for over two decades (Mather and Voyles 2013; Ackerman and Stokes 2003; Stokes and Schwartz 1994). The primary focus of ARM over the past two decades has been on cloud formation processes and their influence on radiative transfer. The advances made in understanding the role of clouds in global climate have been achieved based on the observations from the highly instrumented ground stations around the world. In addition to the fixed ground stations, ARM's deployment of its mobile facilities has enhanced its infrastructure and observational capabilities.

The radar observations of clouds were obtained with vertically pointing Ka-band millimeter-wave cloud radar (MMCR; Moran et al. 1998) and W-band ARM cloud radar (WACR; Widener and Mead 2004). The long-term time–height profiles of clouds provided by MMCR and WACR have been instrumental in better understanding clouds (Remillard et al. 2012; Shupe et al. 2011; Kollias and Albrecht 2010; Protat et al. 2010; De Boer et al. 2009; Kollias et al. 2009; Mace and Benson 2008; Kollias et al. 2007b; Dong and Mace 2003). However,

Corresponding author address: Pavlos Kollias, Department of Atmospheric and Oceanic Sciences, Room 945, Burnside Hall, 805 Sherbrooke Street West, Montreal QC H3A 0B9, Canada.
E-mail: pavlos.kollias@mcgill.ca

DOI: 10.1175/JTECH-D-13-00044.1

complete four-dimensional (space–time) characterization of the cloud formation process and cloud dynamics has never been achieved. Parameterizations of clouds form a significant part of uncertainty in global climate models. Although MMCR and WACR provide long-term high-resolution vertical structure of clouds, they are limited to making observations in the time–height domain and are not intended for three-dimensional mapping of clouds (Kollias et al. 2007a).

In 2010–11, the ARM radar infrastructure enhanced its cloud and precipitation observational capabilities through the American Recovery and Reinvestment Act of 2009 (Mather and Voyles 2013). Currently, the ARM radar infrastructure includes dual-frequency scanning cloud radars operating at X band (9.4 GHz), Ka band (35 GHz), and W band (94 GHz). In addition to the scanning cloud radars, the ARM sites feature scanning precipitation radars operating at X band and C band (5.6 GHz). The augmented radar capability will enable researchers to better characterize cloud properties and study cloud–precipitation interaction. The observations from the scanning cloud radars will help in minimizing the uncertainty associated with cloud parameterizations used in global climate models.

The volume of data from these ARM radars is massive compared to the amount produced by the profiling ARM radars, and the data are in need of substantial postprocessing to fully realize their value. In section 2, the general scientific applications of the scanning ARM cloud radars (SACRs) are described, and section 3 discusses the radar specifications. The challenges associated with sampling clouds in 3D are discussed in section 4. The terminology of all SACR scan strategies is defined in section 5, and the first generation of SACR scan strategies, which are designed to address the aforementioned scientific applications, is outlined in section 6.

2. Background

Since the mid-1990s, ARM supported the development and deployment of several MMCRs for the study of clouds. The ARM cloud radars (MMCRs) provide continuous profiling observations of clouds and, combined with radiation measurements, are used to improve the treatment of cloud and radiation physics in numerical models, including global climate models (Kollias et al. 2007a). The MMCR measurements help to significantly advance our understanding of cloud properties (boundaries, layering, particle phase and size, turbulence) over the last 20 years. These advancements were accompanied by the development of a comprehensive suite of cloud retrieval algorithms using profiling cloud radar and complimentary measurements from lidars and radiometers.

Continuing to operate profiling cloud radars remains a core objective of ARM. Recent enhancements to the radar hardware (Mather and Voyles 2013) have substantially improved the quality of the Ka-band ARM zenith radar (KAZR, replaces the old acronym MMCR) measurements. This is especially true for the quality of the recorded radar Doppler spectra that is expected to provide unique insights into cloud-scale processes (e.g., Kollias et al. 2011a,b). The new KAZR capabilities combined with the addition of profiling precipitation radars at the ARM sites (Tridon et al. 2013b) are expected to strengthen the radar profiling measurements at the ARM sites. The aforementioned improved profiling radar measurements at the ARM sites provide the observational power required to probe clouds and precipitation in the column and be an invaluable source of information for studying cloud-scale processes.

Despite the improvements in the ARM radar profiling measurements, looking only vertically is like looking at cloud systems through a tiny keyhole, thus hiding all the holistic connections. Also, looking only vertically drastically limits opportunities for observing precipitation. All this points to the need for new radars that scan in 3D rather than just pointing vertically, and for radars that can detect precipitation without being blocked by it. Thus, it is important that the ARM observations evolve beyond the 1D ''soda straw'' view of clouds and as a result they can contribute to the cloud parameterization problem within the context of cloud resolving models (CRMs) and large-eddy simulation (LES). Outstanding scientific objectives that require 3D mapping of clouds and precipitation include those listed in the following three subsections.

a. 3D radiative transfer issues, including calculation of radiative flux profiles

As long as cloud structure must be extrapolated from vertically pointing instruments, there will always be an irreducible and unknown uncertainty in comparisons of radiation models with measurements. Thus, computation of instantaneous radiative fluxes for broken and complex cloud fields over the ARM sites would benefit from the information provided by scanning radars, assuming that scanning radars can detect cloud optical depths and cloud boundaries with accuracies approaching the vertically pointing cloud radars. Descriptions of 3D cloud structures would have a significant impact on performing realistic radiative transfer calculations. In particular, scanning cloud radar observations would provide better information on 3D cloud overlap conditions and cloud field anisotropy for the fraction of clouds detected, thus providing tighter constraints on radiative transfer calculations than are derivable from soda-straw data.

TABLE 1. Deployment of SACRs at the ARM sites.

Radar/Site	SGP	NSA	TWP-Darwin	TWP-Manus	AMF-1	AMF-2	Azores	Oliktok
X/Ka-SACR	☐	☐	☑	☑	☐	☑	☐	☐
Ka/W-SACR	☑	☑	☐	☐	☑	☐	☑	☑

Even the smallest amounts of condensed water—for example, a few blobs of altocumulus—are important for radiation fluxes at the few watts per square meters level; hence, this application requires that all clouds be detected in a domain of at least 10-km radius around the ARM Southern Great Plains (SGP) Central Facility.

b. Life cycles of clouds and convective systems and cloud–aerosol interactions

The temporal and spatial scales of both LES and CRMs are suitable for studying cloud life cycles and cloud–aerosol interactions. LES domains are typically 5–6 km with grid spacing of 50 m × 50 m × 50 m. CRMs have much larger spatial domain sizes (i.e., 150–200 km) with 1–2-km grid spacing. LES and CRMs provide one pathway to parameterization development and hence improvement of climate models, and ARM has invested heavily in this pathway. Scanning-radar observations over a 20-km cylinder around the ARM SGP Central Facility could play a vital role in testing and improving LES models and CRMs.

Our current soda-straw observations are severely dimensionally challenged when it comes to testing and evaluating the verisimilitude of LES models and CRMs. Soda-straw observations do not allow us to follow the cradle-to-grave life cycle of individual clouds or cloud systems, and thus they provide no way to evaluate the net result of the various aerosol indirect effects, each of which operates in different stages of a cloud's lifetime. Cloud life cycle studies require detailed observations of all phases of cloud evolution, from initiation, to development of updrafts and downdrafts, to hydrometeor evolution in time and space, to partitioning of condensate into precipitation and outflow anvils.

c. Evaluation of satellite retrievals of cloud system properties

Surface- and satellite-based cloud products, together, are what are available today for evaluating models of all types, but clearly modelers have preferred the satellite data, since it provides the 3D spatial extent and holistic view unavailable in soda-straw data. Typical satellite cloud retrievals rarely have spatial resolution better than 500 m (much worse in the microwave). The soda-straw data are very hard to compare with such satellite data because of the "beam-filling problem"—the problem that ARM's soda-straw measurements refer to only a part, often a small part, of a satellite pixel. A scanning system would allow for observing many satellite and model pixels at the same time, allowing a coherent holistic view rather than our current peek through a keyhole. A scanning system will also enable comparisons with higher statistics of the satellite data unavailable in a soda-straw view (e.g., the spatial correlations among cloud pixels that are so evident to the eye).

3. SACRs

The SACRs are deployed at the four fixed and two mobile ARM facilities. The four fixed ARM sites are the SGP site in Oklahoma; the North Slope of Alaska (NSA) in Alaska; the tropical western Pacific (TWP-Darwin) in Darwin, Australia; and tropical western Pacific (TWP-Manus) on Manus Island, Papua New Guinea. The ARM Mobile Facility 1 and 2 (AMF1 and AMF2, respectively) are deployed around the world for targeted measurement campaigns. Two more SACRs are being developed for the new ARM fixed site at Graciosa Island, Azores, and Oliktok Point, Alaska. The scanning cloud radars will be operated in pairs as dual-frequency radars with the scanning controlled by a single pedestal. This single-pedestal configuration enables simultaneous observations of the cloud field with two widely separated frequencies. Table 1 shows the distribution of the cloud radars at different ARM facilities (fixed and mobile sites) and Table 2 lists the specifications of X-band SACR (X-SACR), Ka-band SACR (Ka-SACR), and W-band SACR (W-SACR).

a. Ka/W-SACR

The Ka- and W-band radar systems mounted on a single pedestal form the dual-frequency scanning cloud radar as shown in Fig. 1. The Ka/W-SACR is mostly intended for midlatitude and Arctic regions where the impact of attenuation (atmospheric water vapor) is less severe than in the tropics. The Ka/W-SACR uses a high-gain and narrow-beam antenna for both frequencies. The beam of the Ka-band and W-band radars are not matched to each other but are very narrow (less than 0.33°) and are suited for cloud observations.

The pedestal is capable of full 360° motion in azimuth and 0°–180° coverage in elevation angle. Ka/W-SACR uses a relatively high-power extended interaction klystron amplifier (EIKA) transmitter with peak power

TABLE 2. Specification of SACRs.

Parameter	W-SACR	Ka-SACR	X-SACR
Transmitter			
Type	EIKA	EIKA	TWTA
Center frequency (MHz)	93 930	35 290	9730
Peak power output (kW)	1.7	2.2	20
Duty cycle (%)	1.0	5.0	1.0
Max pulse width (μm)	1.6	13.0	40.0
Transmit polarization*	H	H	H+V
Max PRF (kHz)	20.0	10.0	10.0
Antenna and pedestal			
Antenna size (m)	0.9	1.82	1.82
3-dB beamwidth (°)	0.30	0.33	1.20
Gain (dB)	54.5	53.5	42.3
Max scan rate ($^\circ s^{-1}$)	36	36	36
Receiver			
Analog/digital (bits)	16	16	16
Receiver polarization	H+V	H+V	H+V
Noise figure (dB)	6.0	5.0	4.5
Sampling rate (MHz)	120	120	120
Decimation factor	Adj	Adj	Adj
Video bandwidth	Adj	Adj	Adj
Sensitivity** (dBZ at 5 km)	−17.1	−20.9	−5.0

* H denotes horizontal polarization, H+V denotes simultaneous horizontal and vertical polarization, and Adj stands for adjustable.

** 333-ns single-pulse sensitivity.

over 1.6 kW (Table 2). The receiver and the transmitter units are antenna mounted, which results in low loss in the radar front end. The total loss in the W-SACR is significantly more than the losses in Ka-SACR, which degrade the sensitivity of W-SACR. However, a small design modification and component upgrade for W-SACR is planned, which will negate the high front-end loss currently experienced in W-SACR. The Ka- and W-band systems are dual-polarization radar systems, which only transmit horizontal polarization state but receive signals in both horizontal and vertical polarization states. Both the Ka- and W-band radars shall provide linear depolarization ratio (LDR) observations down to −30 dB or better (limited by the antenna cross-polarization isolation), which are useful for habit identification in ice clouds (Table 2). The Ka/W-SACR uses an arbitrary digital waveform generator, which enables the use of frequency diversity and pulse compression waveforms for operations. The SACR uses spectral processing for filtering and parameter estimation. The system routinely stores the full Doppler spectrum when operating in zenith-pointing mode and is capable of storing the base-band in-phase and quadrature-phase signals. The Ka/W-SACR uses a corner reflector target located on a tower at a range of 400–500 m. The SACR can be remotely configured and has been designed to be able to interface with algorithms to set adaptive scanning.

b. *X/Ka-SACR*

The X-band and Ka-band radar systems mounted on a single pedestal form the dual-frequency scanning cloud radar as shown in Fig. 1. The X/Ka-SACR is mostly geared toward tropical regions where the atmospheric water vapor will not have a severe impact on X and Ka bands, whereas attenuation at W band is severe. The beams of the X- and Ka-band radars are not matched to each other. The X-SACR uses a much wider beam (about 3.5 times wider) compared with Ka-SACR. Mounting an X-band antenna with a beamwidth comparable to that of Ka-SACR (0.33°) on the same pedestal was not practically viable. The X/Ka-SACR pedestal/control is identical to that of Ka/W-SACR and therefore has the full range of motion in azimuth and ±0°–180° coverage in elevation angle. The X-SACR uses a relatively low-peak-power traveling wave tube (TWT) transmitter but is sensitive enough to observe drizzle and light rain (Table 2). The receiver and the transmitter units are antenna mounted, which results in low loss in the radar front

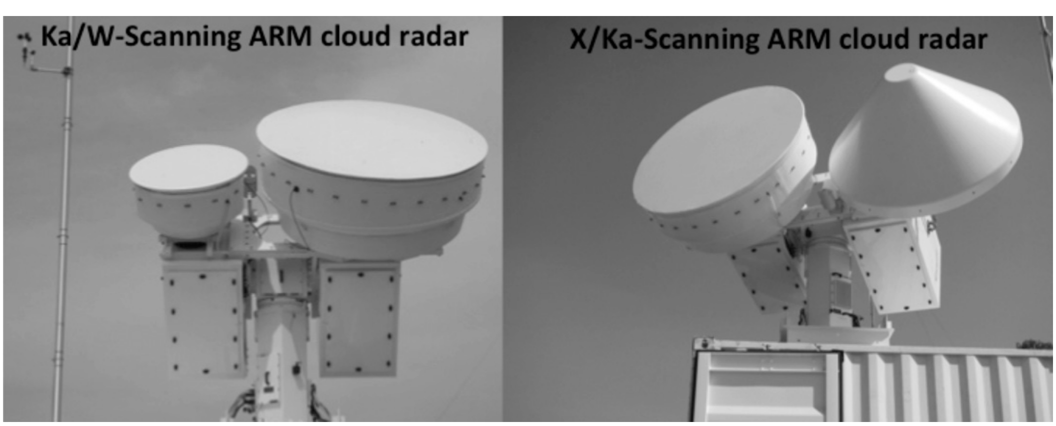

FIG. 1. Photographs of the dual-frequency SACR, showing the (left) Ka/W-SACR and (right)X/Ka-SACR systems.

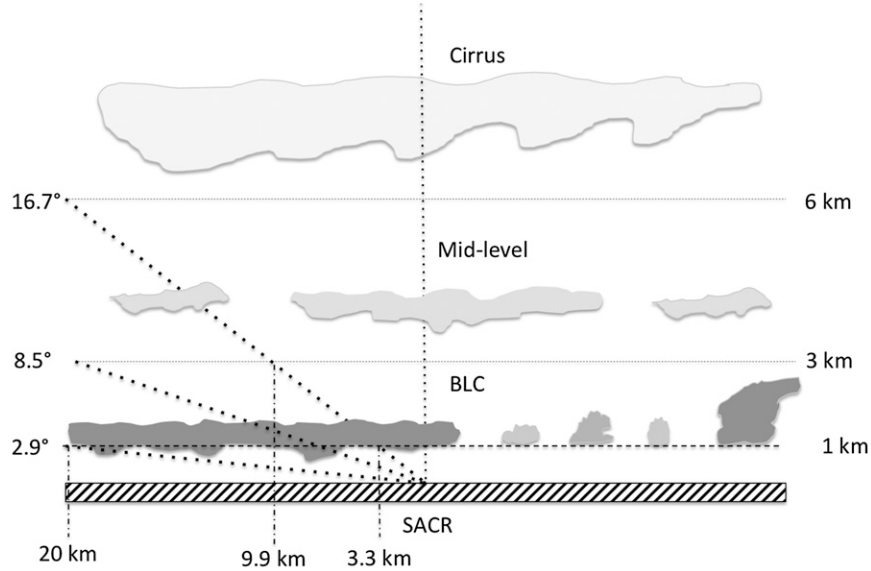

FIG. 2. Schematic of different cloud conditions and SACR scanning geometry.

end. The X-band system is a fully polarimetric radar system that simultaneously transmits and receives signals in horizontal and vertical polarization (Table 2). The X-band system shall not provide any cross-polarization observations. The Ka-band system is a dual-polarization radar system that only transmits the horizontal polarization state but receives the signals in both horizontal and vertical polarization states. The Ka-band radar shall provide LDR observations. In the absence of precipitation radar in the vicinity of the AMF-2 deployment, the X-band system can be deployed on a separate pedestal. The waveform generator, digital receiver, and signal processor are identical to Ka/W-SACR and maintain all the features listed in the previous section.

4. Challenges in sampling cloudy atmospheres

Scanning clouds in three dimensions has never been done in a continuous operating environment. Cloud structures and volumes are vastly different for rain and snow shafts, which are the primary targets of precipitation radars. While scientists expect to reuse many of the ideas implemented in scanning weather radar systems, the need to detect both low- and high-level stratiform clouds, broken clouds, multilayer cloud conditions, and associated precipitation requires new sampling approaches.

The cloud systems are volume targets that are distributed over a large area. ARM has made observations of cloud systems with a zenith-pointing radar for more than a decade. The zenith-pointing radars have provided vertical profiles of the cloud properties. The deployment of scanning cloud radars will enable the observation of a cloud system in a spatiotemporal context. Traditionally, scanning weather radars make observations with volume coverage patterns (VCP) made up of plan position indicator (PPI) scans at several elevation tilts. Three-dimensional observations of cloud systems pose a few challenges that must be taken into account for designing scan strategies.

a. Spatial resolvability

The spatial structure of cloud systems varies considerably when compared to large-scale precipitating cloud systems. Precipitating systems tend to have continuous spatial structure—especially in the vertical column—when compared to the ''suspended'' layered and broken nature of clouds. The SACR scan strategies need to provide adequate description of cloud systems that have continuous spatial structure in the lower and upper troposphere (e.g., cirrus and stratus clouds) and at the same time provide observation of discrete broken clouds with sufficiently fast temporal update so their temporal evolution can be monitored. In addition, the vertical extent of clouds can vary from very thin single-layer clouds, to multiple cloud layers, to thick cloud structures (Fig. 2). Observations must be made at scales on the order of 100 m to several kilometers. The requirements to (i) maintain small radar sampling volumes at ranges up to 20 km, (ii) make matched-beam dual-wavelength measurements at Ka and W bands, and (iii) collect high-quality radar Doppler spectra in profiling mode led to narrow antenna beamwidths for the Ka- and W-band SACR systems (0.33° and 0.3°, respectively; Table 2).

The nominal operational pulse repetition frequency (PRF) of the Ka-SACR is 5 kHz, which limits the operational range of the radar to 30 km. In fact, currently ARM samples (digitizes) the first 20 km. The 5 kHz is imposed by the need to avoid severe velocity aliasing due to the horizontal wind contribution to the observed Doppler velocities. Another reason to limit the usable range of the SACR to 20 km is the fact that its sensitivity drops below −20 dB*Z* at 20 km.

b. Geography

The geographical location of the radar deployment has a significant role in the development of scan strategies for cloud radars. The climatology and atmospheric conditions vary from Arctic regions, midlatitude regions, and tropical regions. In addition to climatology and atmospheric conditions, the geolocation of the radar close to oceans is an important consideration. For example, the land, ocean, and land–ocean boundary have to be adequately observed. Such scenarios must be taken into account while considering scan strategies.

c. Cone of silence

Weather radar VCPs typically consist of a series of azimuthal scans (PPI) at fixed elevations (7–15 different elevation angles) with most of the elevations at very low angles (0.5°–10°) and a maximum elevation angle near 20°. This sampling strategy is optimum to detect and monitor weather at long ranges (100–400 km). However, it generates a cone of silence (absence of radar observations) centered over the radar location and for angles higher than 20°. For example, at the 20-km range, PPI scans at 2.5°, 8.5°, and 16.7° will generate a cone of silence at heights 1, 3, and 6 km, respectively. This implies that if we selected a VCP with a maximum elevation of 16.7°, no clouds above 6-km height will be detected within a 20-km radius from the SACR location. For the same maximum elevation angle, clouds above 3 and 1 km will not be detected within a 9.9- and 3.3-km radius from the SACR location. This is not an issue for operational weather radars, since they are typically offset several kilometers from the main areas of interest (e.g., metropolitan areas, storms of interest) and their observations cover hundreds of kilometers; the cone of silence has little or no effect on the operational weather radar objectives. On the contrary, each fixed or mobile ARM site is equipped with a large number of active and passive instruments that provide measurements related to aerosols, radiation, cloud properties, surface meteorology, and thermodynamic profiling. Most of these sensors operate in a profiling mode to provide a complete characterization of the overlying column with a typical field of view from a fraction of a degree to hemispherical (e.g., broadband radiometers, total-sky imager). The vast majority of photons received by the sensors are coming from the part of the sky that typical weather radar VCPs will not sample (Fig. 2). Furthermore, the SACRs are collocated with, rather than offset by, several kilometers from the ARM fixed and mobile sites. Thus, connecting the SACR observations with 3D cloudy atmosphere radiative transfer problems requires that the SACR sample the cone of silence over the ARM sites.

TABLE 3. SACR operating mode.

Parameter	W-SACR	Ka-SACR	X-SACR[a]
Transmit polarization[b]	H	H	H+V
Receive polarization[b]	H+V	H+V	H+V
PRF (kHz)	5.0 (9.058[c])	5.0	TBD
Pulse width (μm)	1.6	3.0	TBD
Nyquist velocity (m s^{-1})	4.0 (7.22[c])	10.6	TBD
Scan speed (deg^{-1})	9.0	9.0	9.0
Effective beamwidth (deg)	0.43	0.43	TBD
Gate spacing (m)	25	25	TBD
FFT length	64 (256[c])	64 (256[c])	TBD
No. of spectral averages	3 (70[c])	3 (40[c])	TBD
Sensitivity[d] (dB*Z* at 5 km)	−21.2	−27.8	TBD

[a] Not operational yet.
[b] H denotes horizontal polarization; H+V denotes simultaneous horizontal and vertical polarization.
[c] Zenith-pointing mode.
[d] Pulse compression waveform single-pulse sensitivity.

d. Scan-rate limitations

Traditionally, ARM zenith-pointing profiling radars use large antennas, implement various transmit waveforms to cover the lower and upper troposphere, and integrate thousands of samples to improve sensitivity using spectral methods (Moran et al. 1998; Kollias et al. 2007a). The scanning Ka-SACR, despite its sophisticated design, the use of high-power klystron transmitters, and the use of pulse compression, are not as sensitive as the vertically pointing ARM cloud radars. Additionally, the primary objective of the SACR systems is the objective determination of 3D cloudiness above a radar reflectivity threshold (−30 dB*Z* at 10-km range). This requires the estimate of radar Doppler moments of clouds at low signal-to-noise conditions. Extracting low uncertainty Doppler moments at low signal-to-noise conditions requires signal integration. Currently, the SACR moments are based on three 64-FFT-point spectra averages (a total of 192 sample integrations; Table 3). With an operational PRF of 5 kHz, and an antenna beamwidth of 0.33° (Table 3), the antenna scan rate is limited to 9° s^{-1}. Therefore, scan speed, volume update time, and sensitivity are constrained by the very narrow beamwidth. As a result, the SACR scanning rate is considerably slower than that employed by operational and research weather radar, and this must be considered in the sampling mode design.

e. Volume coverage trade-off

The aforementioned challenges suggest that a VCP with PPIs concentrated in the low elevation will be ineffective in capturing the structure of cloud systems because of the use of a narrow beamwidth, the need to sample the cone of silence and the nature, variability, and altitude of clouds. A VCP with PPIs spaced in elevation to cover higher elevations could provide cloud information in the cone of silence. There are two shortcomings that make this approach ineffective. First, every PPI requires 40 s to complete ($9° s^{-1}$ scan rate) and a modest number of elevation angles (25–30) are required to address sampling of shallow cloud layers, especially in the boundary layer. This leads to a VCP sampling time of 13–17 min, which is deemed as too long to assume stationary cloud conditions as a necessary condition to reconstruct the 3D cloud field. For example, assuming a low horizontal wind speed of $20 m s^{-1}$ in the upper troposphere, clouds above 6 km will have advected 16–20 km in the SACR sampling volume within the same VCP. Second, the reconstruction of a 3D cloud field from such a high-elevation-angle VCP is challenging due to the large vertical variability of the clouds. On the other hand, PPI scans can provide great information if used to target specific scientific applications. For examples, PPI scans at 0.5° are useful to map near-surface drizzle structures and PPI scans at 45° can provide valuable polarimetric measurements, especially at the North Slope of Alaska ARM sites. If a network of SACRs is available, then it should be possible to reconstruct 3D cloudy volumes using PPI-based VCP. Nevertheless, the first generation of SACR operating sampling strategies is based mainly on sequences of range–height indicator (RHI) volume scans with the possibility to add a few PPI scans in the surveillance scan (see sections 5 and 6).

5. Generalized scan system nomenclature for SACRs

The three-dimensional mapping of cloud systems is obtained by observations from a combination of scan strategies designed for targeted cloud systems. The scan strategies are governed by the cloud properties and geography of each radar site. Traditional atmospheric radars scan in elevation axis (RHI) and azimuth axis (PPI). Although RHI and PPI scans encompass all the basic scans of atmospheric radars, the scanning nomenclature for ARM's cloud and precipitation radar observation is decomposed into a number of elemental scan segments. These elemental scan segments are designated for targeted cloud and precipitation systems. In addition, a calibration-specific elemental scan segment is defined as a part of ARM's scan nomenclature.

An individual scan segment is represented as $S_x(T_x)$, where the subscript x indicates the nature of the scan for a targeted purpose and T_x is the time duration of the observation associated with the elemental scan segment. The elemental scan segments can be grouped into a set to form a targeted scan strategy for the radars. ARM's scan nomenclature is also used to name and archive the data files generated by the radars. This nomenclature also facilitates the organization and development of ARM's value-added products (VAPs). The following sections describe the elemental scan segments used in developing scan strategies for ARM scanning radars.

a. PPI

The PPI scan segment S_p is defined as

$$S_p(T_p) \equiv \{s(\theta_{e1}, \Delta\phi_a), s(\theta_{e2}, \Delta\phi_a), \ldots, s(\theta_{en}, \Delta\phi_a)\}, \quad (1)$$

where $s(\theta_{en}, \Delta\phi_a)$ is the nth full 360° or sector sweep $\Delta\phi_a$ at a constant elevation angle θ_{en}. Figure 3a shows an illustration of S_p with four sweeps.

b. RHI

The RHI scan segment S_r is defined as

$$S_r(T_r) \equiv \{s(\phi_{a1}, \Delta\theta_e), s(\phi_{a2}, \Delta\theta_e), \ldots, s(\phi_{an}, \Delta\theta_e)\}, \quad (2)$$

where $s(\phi_{an}, \Delta\theta_e)$ is the nth RHI sweep at an azimuth angle ϕ_{an} and sweeping $\Delta\theta_e$ from zero elevation angle. Figure 3b shows an illustration of three S_r segments.

c. Vertically pointing profiles (VPT)

In the VPT [S_v (T_v)] mode, the antenna is in a fixed position pointing vertically. Both moments and spectra are stored. The VPT mode is predominantly used for dual-wavelength radar Doppler spectra measurements of the column with the goal of improving cloud property retrievals. The radars will operate in VPT mode for 15–30 min. Figure 3c shows an illustration of several S_v segments.

d. CRCAL

A corner reflector is used for calibration purposes. The corner reflector can be used for cloud radar calibration because the very narrow beam of the cloud radars provides very good signal-to-clutter ratio. The corner reflector calibration profiles (CRCAL) $S_{CR}(T_{CR})$ can be obtained by pointing the antenna in the direction

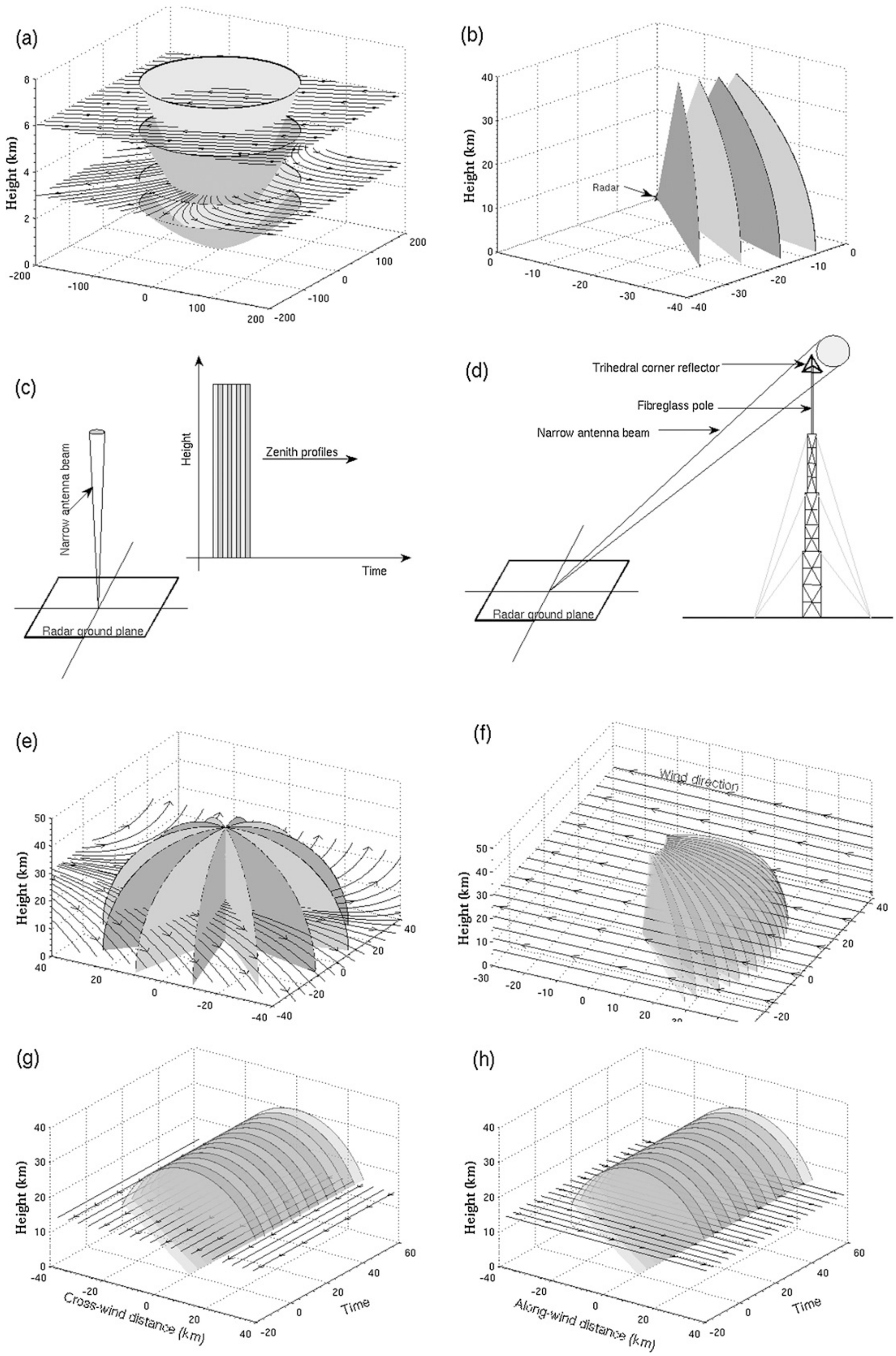

FIG. 3. Schematic representation of different SACR scanning modes: (a) PPI, (b) RHI, (c) VPT, (d) CRCAL, (e) HSRHI, (f) BLRHI, (g) CWRHI, and (h) AWRHI.

of the fixed corner reflector. Figure 3d shows an illustration of $S_{\rm CR}$ segments.

e. Hemispheric sky RHI (HSRHI)

The horizon-to-horizon scan segment S_h is defined as

$$S_r(T_r) \equiv \{s(\phi_{a1}, \Delta\theta_e = 180), s(\phi_{a2}, \Delta\theta_e = 180), \ldots, s(\phi_{an}, \Delta\theta_e = 180)\}, \quad (3)$$

where $s(\phi_{an}, \Delta\theta_e = 180)$ is a 0°-to-180° RHI sweep (horizon to horizon) at azimuth ϕ_{an}. A total of n horizon-to-horizon RHI sweeps are performed at different azimuth angles. Figure 3e shows an illustration of S_h scan with $n = 6$. The HSRHI mode is to assist the study of climatology of cloud systems. Currently, the HSRHI implemented at the SACR uses $n = 6$ and the horizon-to-horizon scans are spaced by $\Delta\phi = 30°$. This volume scan takes approximately 2–3 min, including the time overhead for the SACR positioner.

f. Boundary layer RHI (BLRHI)

The boundary layer scan segment S_b is defined as

$$S_b(T_b) \equiv \left\{\Delta\theta_b = \theta_{\rm start} - \theta_{\rm end}, \phi_b = \phi_c - \frac{\phi_T}{2}{:}\, \Delta\phi_a{:}\, \phi_c + \frac{\phi_T}{2}, s_r(\phi_b, \Delta\theta_b)\right\}, \quad (4)$$

where $S_b(T_b)$ is an RHI volume with sweeps from elevation angle $\theta_{\rm start}$ to $\theta_{\rm end}$ (currently set from horizon to zenith) with the RHI sweeps separated by $\Delta\phi_a$ (currently set to 2°) in azimuth, ϕ_T is the total azimuthal spread (currently set to 80°), and ϕ_c is the azimuth angle at the center of the RHI volume sector; ϕ_c is chosen to be collinear to the mean wind direction in the cloud layer of interest. The wind direction varies with the altitude and should be selected carefully based on climatology and the nearest (in time) atmospheric sounding data (section 5). Figure 3f shows an illustration of an S_b scan. The primary objective of the BLRHI mode is to enable the study and characterization of the life cycle and evolution of cloud systems. The time duration of the BLRHI volume scan is constraint to a maximum of 5 min and this affects mainly the selection of the $\theta_{\rm end}$.

g. Crosswind RHI (CWRHI)

The crosswind RHI scan segment S_c is defined as

$$S_c(T_c) \equiv \{\phi_c, \Delta\theta_c = \theta_{\rm start} - \theta_{\rm end}, s_r(\phi_c, \Delta\theta_c)\}, \quad (5)$$

where $s_r(\phi_c, \Delta\theta_c)$ is a repeated RHI scan performed at an azimuth angle ϕ_c that is orthogonal to the mean wind direction in the cloud layer of interest. The sweeping elevation angle $\Delta\theta_c$ starts at $\theta_{\rm start}$ (currently set to 0°) and ends at $\theta_{\rm end}$ (currently set to 180°). Figure 3g shows an illustration of an S_c segment. The objective of the CWRHI mode is to document the 3D structure of cloud systems as they advect over the SACR location. Currently, the radars are set to operate in CWRHI mode for $T_c = 25$ min that results to 60–70 sets of RHI scans within a CWRHI.

h. Along-wind RHI (AWRHI)

The along-wind RHI scan segment S_a is defined as

$$S_a(T_a) \equiv \{\phi_a, \Delta\theta_a = \theta_{\rm start} - \theta_{\rm end}, s_r(\phi_a, \Delta\theta_a)\}, \quad (6)$$

where $s_r(\phi_a, \Delta\theta_a)$ is a repeated RHI scan performed at an azimuth angle ϕ_a that is aligned with the mean wind direction in the cloud layer of interest. The sweeping elevation angle $\Delta\theta_e$ starts at $\theta_{\rm start}$ and sweeps back to $\theta_{\rm end}$. Currently, $\Delta\theta_e$ is set to 180°. Figure 3h shows an illustration of an S_a segment. The antenna is pointing at θ_a, which is along or aligned with the direction of the wind. The objective of the AWRHI mode is to enable cloud lifetime studies during periods of weak directional shear in the cloud layer of interest. The AWRHI enables monitoring cloud systems as they move close to, over, and away from the SACR location (Borque et al. 2013, manuscript submitted to *J. Appl. Meteor. Climatol.*). Currently, the radars are set to operate in AWRHI mode for $T_a = 25$ min that results to 60–70 sets of RHI scans within an AWRHI.

6. First-generation SACR operational modes

The ability to observe cloud systems in a spatial–temporal context is challenged by the geometrical characteristics of cloudy atmospheres and limited by the scanning parameters of the SACRs (see section 4). It is apparent that a single-scan pattern cannot be used to observe and characterize the cloud systems that exist in nature. Therefore, it is necessary to combine targeted scans to form an ensemble scan pattern that will enable observations of cloud systems in an operational environment. It is important to design a first-generation scan strategy that will provide measurements necessary to retrieve cloud properties that are directly relevant to the ARM scientific objectives (see section 2). The first-generation scan strategy will also serve as a framework to develop a long-term scan strategy that will ultimately benefit long-term climate research.

The objective of the first generation of the SACR scan strategy is to collect 3D cloud structure statistics and to

TABLE 4. SACR scan strategies.

Scan strategy	Description	Duration (min)
HSRHI+PPI	A combination of six horizon-to-horizon RHIs at six azimuth angles spaced by 30°, followed by a 360° low-level PPI at 0.5° elevation.	5
CWRHI	A set of 60–70 repeated horizon-to-horizon RHI scans with the radar scan plane set perpendicular to the mean wind direction in the cloud layer.	25
AWRHI	A set of 60–70 repeated horizon-to-horizon RHI scans with the radar scan plane set parallel to the mean wind direction in the cloud layer.	25
BLRHI	Five sets of 90° azimuth sector volume scans with the center of the volume scan aligned with the mean wind direction in the boundary layer. Each volume scan is composed of 40–45 horizon-to-zenith RHI scans.	25
VPT	Vertically pointing observations with Doppler spectra recording.	25

improve cloud microphysical and dynamical retrievals. A complete cycle of SACR scan modes is developed using six elemental scan segments to address various observational needs (Table 4). A low-level PPI scan and HSRHI scan (hereafter HSRHI+PPI scan) is used on a regular basis, as a reference mode, to build cloud statistics in the coverage region of the radar. The HSRHI+PPI scan is completed in 4–5 min and is repeated every 30 min. It can be seen as the climatology SACR mode. The HSRHI portion of the scan is designed to provide horizon-to-horizon RHI cross sections of the cloud and precipitation conditions at six fixed azimuthal directions spaced by 30°. The HSRHI scan provides range–height information of cloud occurrence and layering in six different azimuth directions. The RHI scans can provide information of the anisotropy and variability of the cloud field with respect to environmental conditions (e.g., wind direction). A sequence of these scans (available every 30 min) can be used to monitor cloud field advection over the ARM sites. Furthermore, the Doppler velocity measurements collected during the HSRHI scan can be used to retrieve the in-cloud horizontal wind field. The low-elevation PPI scan is designed to characterize the cloud and precipitation conditions near the surface in a radius of 20 km around the ARM sites.

Between HSRHI+PPI scans, there are 25–26 min that are dedicated to different scan modes (CWRHI, AWRHI, VPT, and BLRHI Fig. 4). The CWRHI scan is repeated 60–70 times within 25 min (scan rate of $9° s^{-1}$) and is designed to slice cloud structures in a crosswind plane, enabling the reconstruction of cloud structures in a Cartesian coordinate system, where the coordinates are radar scan plane, height, and time. The AWRHI scan strategy is also repeated 60–70 times within a 25-min period and aims to provide observations of the same cloud volumes as they approach, move over, and move away from the ARM site. The success of this scan strategy critically depends on the wind directional shear within the cloud layer of interest. The field of view of the SACR is narrow (0.3°) and the directional shear can result in the observation of new cloud volumes from one RHI to the next and thus does not allow the study of the temporal evolution of the same volume. This is also the challenge if the AWRHI scan is not well aligned with the wind direction (Borque et al. 2013, manuscript submitted to *J. Appl. Meteor. Climatol.*). The BLRHI scan aims to document the 4D evolution of clouds, monitoring in time the 3D cloud structure (especially boundary layer broken cumuli). Because of the wider azimuth sector (90° rather than one azimuth angle), the BLRHI scan strategy is more tolerant to small wind direction changes within the cloud layer. The disadvantage is that the full sector volume scan requires 5 min to be completed; thus, it can be repeated 5 times. The current spacing of 2° between the azimuths of the horizon-to-zenith RHI planes translates to ~350 m at 10-km distance of the radar. Based on the analysis of ground-based radar observations, 350-m resolution is sufficient to sample shallow cumuli clouds. The VPT vertically pointing observations are critical for strengthening column retrievals using spectral and dual-frequency retrievals. The Ka- and W-SACR feature similar antenna beamwidth, and temporal and spatial sampling, and should in principle offer high-quality dual-wavelength observations of clouds (Tridon et al. 2013b). The entire scan sequence for the first-generation SACR operations (Table 4) is given by

$$S(T) = \left\{ \begin{array}{l} [S_p(T_p), S_h(T_h)], S_c(T_c)[S_p(T_p), S_h(T_h)], S_a(T_a), \\ [S_p(T_p), S_h(T_h)], S_v(T_v)[S_p(T_p), S_h(T_h)], S_b(T_b) \end{array} \right\}. \tag{7}$$

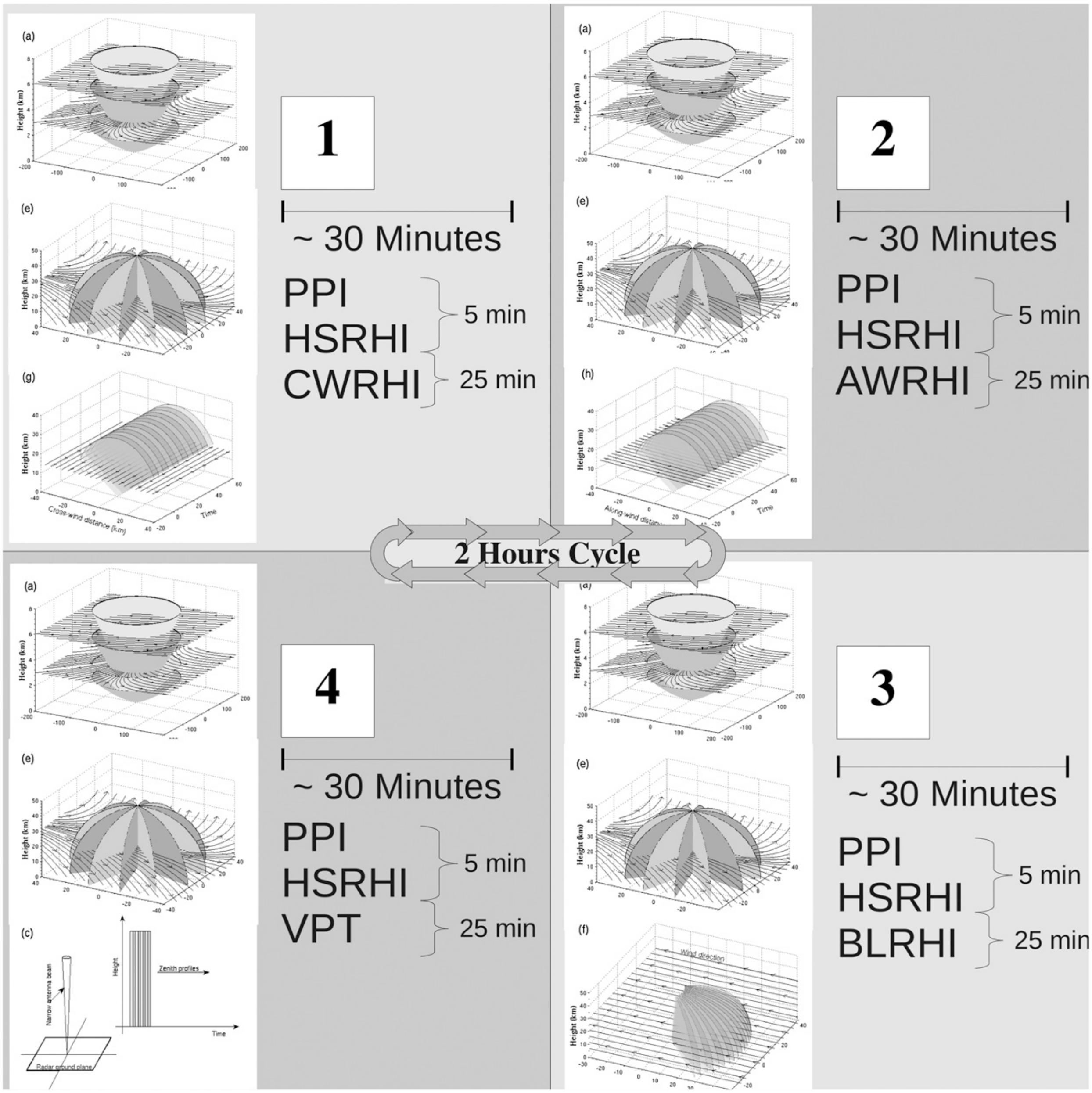

FIG. 4. A 2-h SACR scanning mode sequence.

The total time for a single cycle is $T = 2\,\mathrm{h}$, $T_p + T_h \approx 5\,\mathrm{min}$, and $T_c = T_a = T_v = T_b \approx 25\,\mathrm{min}$. The 2-h scan cycle is shown in Fig. 4. The salient parameters used in the operating mode for SACR are listed in Table 3, and the descriptive summary of the current SACR modes is provided in Table 4. The scan rate for all the scanning modes is set to $9^\circ\,\mathrm{s}^{-1}$, and the integration cycle while scanning uses 192 pulses. The spectral processing uses a 64-point FFT to compute the power spectral density, and three spectral averages are performed per range gate.

The effective beamwidth due to scanning exceeds the beamwidth by about 0.1°. The number of spectral averages and spectral points changes for the vertically pointing mode. A 256-point FFT is used in the vertically pointing mode with 70 and 40 spectral averages in W-SACR and Ka-SACR, respectively. Both the W-SACR and Ka-SACR transmit a long pulse with a chirp waveform. The long pulse increases the average power and thereby improves sensitivity. It is important to note that the sensitivity listed in Table 3 is for a single pulse. The additional gain of 3–10 dB in sensitivity due to spectral

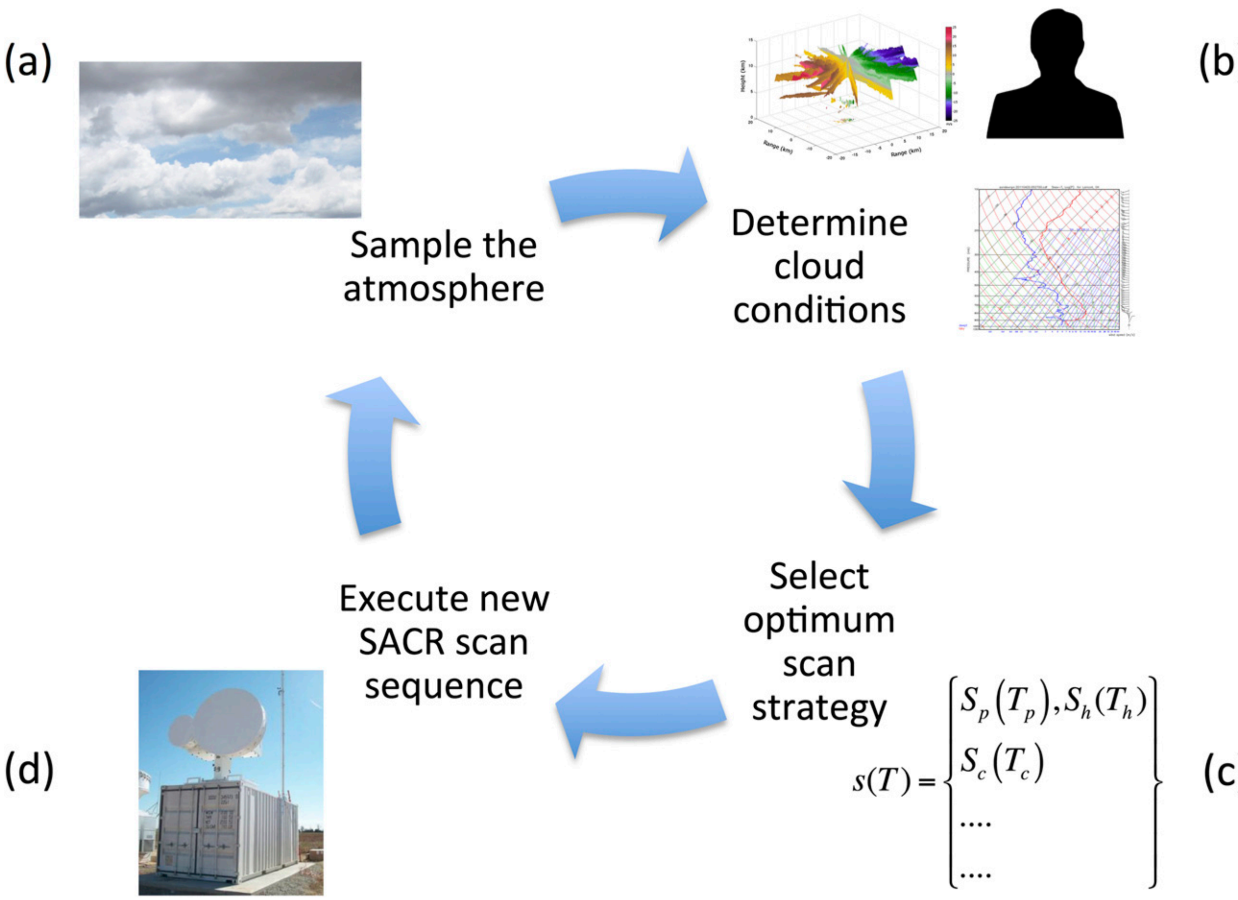

FIG. 5. Illustration of adaptive SACR sampling strategy cycle: (a) The SACR and other ARM instruments (e.g., sounding, lidar, disdrometer) sample the atmosphere, (b) the observations and/or field experts (e.g., PI) determine the atmospheric cloud state (e.g., cloud fraction with height, wind direction, precipitation occurrence), (c) the output of the analysis (automated or PI driven) is used to determine the optimum scan strategy, and (d) the new SACR scan sequence is executed. This cycle will lead to another period of atmospheric sampling and the cycle is repeated.

processing is dependent on the Doppler spectral width that determines the signal decorrelation and thus the number of independent samples.

The wide scope of scientific objectives that needs to be addressed by SACR observations suggests that the SACR scan strategies should be capable of being altered to focus on any cloud system from deep anvil clouds to shallow stratus. Such versatility would require flexibility and adaptive operational modes implemented by the ARM radar operations groups for each individual SACR instrument and for the ARM radar facility (combined cloud and precipitation radars at each site) as a whole. The first-generation SACR scan strategies described here are considered to be equivalent to the ‘‘*sit and spin*’’ mode in the case of scanning radars. In the sit-and-spin strategy, the radars perform predefined sampling strategies independent of the evolving cloud conditions and experiment. This approach is popular, since it produces standard data files and products that do not change.

The second approach is known as ‘‘*adaptive*,’’ where the radar sampling strategy is defined either by the principal investigators (PIs) in the field in coordination with the ARM radar operations group during intensive observation periods to best serve the scientific objectives of the field campaign or by cloud, precipitation, and horizontal-wind-state detection algorithms that dictate optimal scan strategies for the SACRs in order to sample the atmosphere at the altitudes where clouds are present (Fig. 5). The cloud and wind-state detection algorithms will receive its input from standard ARM data streams (e.g., nearest sounding in time, rainfall rate, ceilometer cloud base) and from the latest SACR HSRHI+PPI observations (Fig. 5b). The input data will be used to determine the cloud fraction, number of cloud layers, height and thickness of hydrometeor layers, the occurrence of precipitation at the ground, and the wind direction as a function of height. In turn, this information will be used to select the optimum scan strategy (Fig. 5c). Possible scan optimizations include adaptively defining wind direction every 30 min in order to ensure the best sampling conditions for the BLRHI, AWRHI, and CWRHI modes as well as replacement of some of the scan modes with the one that is optimum for specific cloud and precipitation conditions. Two such examples are the replacement of the AWRHI and BLRHI with CWRHI and VPT during cirrus clouds conditions and the replacement of AWRHI, BLRHI, and CWRHI with VPT during periods with measurable precipitation at the surface.

In this adaptive mode, the SACR would be somewhat of a chameleon, capable of being configured to target a large variety of cloud and precipitation conditions, and it differs markedly from the traditional approach where instrument sampling strategy is independent of the atmospheric features being sampled (McLaughlin et al. 2009; Zink et al. 2008). The introduction of scientifically driven flexibility in SACR scan strategies has gained traction in ARM, and discussions about the rules and priorities that will determine optimal SACR scan strategies in the future are underway.

7. Summary

ARM operates scanning cloud radars (SACRs) at all fixed and mobile sites. The SACRs are the most sophisticated radar systems at all ARM sites and will become the primary instruments for the detection of cloud properties (boundaries, water content, dynamics, etc.) beyond the soda-straw (profiling) view. The SACR observations are expected to enhance our understanding of the role of cloud inhomogeneity in radiative transfer, to provide information on the 3D structure of cloud systems, to document the temporal evolution of clouds, and to improve dynamical and microphysical retrievals in clouds and precipitation (Lamer et al. 2013).

The SACRs have scanning capabilities with two frequencies and polarization, and thus allow more accurate probing of a variety of cloud systems (e.g., drizzle and shallow, warm rain), better correction for attenuation, use of attenuation for liquid water content retrievals, polarimetric characterization of nonspherical particles, and habit identification.

Determining the scan strategy for the SACRs is challenging. The complexity and variety of cloud scenes, and the geographical distribution of the ARM fixed and mobile sites suggests that more than one sampling mode is required. Contrary to practices applied in weather radar VCPs, the SACRs need to sample the cone of silence. Finally, the narrow beamwidth of the SACRs and the need to have a relatively large number of samples per integration add additional constraints in the selection of the SACR scan strategies.

To address the wide scope of scientific objectives, several scan modes are defined. Most of the scan modes are based on horizon-to-horizon RHI scans that aim to document the atmospheric cloud state in discrete azimuthal planes accounting for the wind direction. The first generation of SACR scan strategies is based on a sequence of six different scan modes (HSRHI, PPI, CWRHI, AWRHI, BLRHI, and VPT) that is completed in 2 h. The HSRHI+PPI scan strategy is used as a reference (climatology) mode and is repeated nominally every 30 min, but this could change to 15 min depending on the deployment and cloud climatology. The other four scan modes are designed for addressing different scientific objectives and rotate in time interleaved with the HSRHI+PPI climatology mode. The first-generation SACR scan strategy is static (sit and spin). In the near future, the SACR scan strategy will be optimized using real-time information about the atmospheric cloud and wind state from auxiliary and SACR observations in a closed-loop process. The proposed SACR scan strategy will be evaluated in the future based on the quality and application of the collected observations. Refinements are expected in the future as we learn more about how to best sample clouds in 3D.

Acknowledgments. This work was supported by the Office of Biological and Environmental Research of the U.S Department of Energy (as part of the Atmospheric Radiation Measurement Climate Research facility).

REFERENCES

Ackerman, T. A., and G. M. Stokes, 2003: The Atmospheric Radiation Measurement Program. *Phys. Today,* **56,** 38–45.

De Boer, G., E. W. Eloranta, and M. D. Shupe, 2009: Arctic mixed-phase stratiform cloud properties from multiple years of surface-based measurements at two high-latitude locations. *J. Atmos. Sci.,* **66,** 2874–2887.

Dong, X., and G. G. Mace, 2003: Profiles of low-level stratus cloud microphysics deduced from ground-based measurements. *J. Atmos. Oceanic Technol.,* **20,** 42–53.

Kollias, P., and B. A. Albrecht, 2010: Vertical velocity statistics in fair-weather cumuli at the ARM TWP Nauru Climate Research Facility. *J. Climate,* **23,** 6590–6604.

——, E. E. Clothiaux, M. A. Miller, B. A. Albrecht, G. L. Stephens, and T. P. Ackerman, 2007a: Millimeter-wavelength radars: New frontier in atmospheric cloud and precipitation research. *Bull. Amer. Meteor. Soc.,* **88,** 1608–1624.

——, G. Tselioudis, and B. A. Albrecht, 2007b: Cloud climatology at the Southern Great Plains and the layer structure, drizzle, and atmospheric modes of continental stratus. *J. Geophys. Res.,* **112,** D09116, doi:10.1029/2006JD007307.

——, M. A. Miller, K. L. Johnson, M. P. Jensen, and D. T. Troyan, 2009: Cloud, thermodynamic, and precipitation observations in West Africa during 2006. *J. Geophys. Res.,* **114,** D00E08, doi:10.1029/2008JD010641.

——, J. Rémillard, E. Luke, and W. Szyrmer, 2011a: Cloud radar Doppler spectra in drizzling stratiform clouds: 1. Forward modeling and remote sensing applications. *J. Geophys. Res.,* **116,** D13201, doi:10.1029/2010JD015237.

——, W. Szyrmer, J. Rémillard, and E. Luke, 2011b: Cloud radar Doppler spectra in drizzling stratiform clouds: 2. Observations and microphysical modeling of drizzle evolution. *J. Geophys. Res.,* **116,** D13203, doi:10.1029/2010JD015238.

Lamer, K., A. Tatarevic, I. Jo, and P. Kollias, 2013: Evaluation of gridded Scanning ARM Cloud Radar reflectivity observations and vertical Doppler velocity retrievals. *Atmos. Meas. Tech. Discuss.,* **6,** 9579–9621, doi:10.5194/amtd-6-9579-2013.

Mace, G. G., and S. Benson, 2008: The vertical structure of cloud occurrence and radiative forcing at the SGP ARM site as revealed by 8 years of continuous data. *J. Climate,* **21,** 2591–2610.

Mather, J., and J. Voyles, 2013: The ARM Climate Research Facility: A review of structure and capabilities. *Bull. Amer. Meteor. Soc.,* **94,** 377–392.

McLaughlin, D., and Coauthors, 2009: Short-wavelength technology and the potential for distributed networks of small radar systems. *Bull. Amer. Meteor. Soc.,* **90,** 1797–1817.

Moran, K. P., B. E. Martner, M. J. Post, R. A. Kropfli, D. C. Welsh, and K. B. Widener, 1998: An unattended cloud-profiling radar for use in climate research. *Bull. Amer. Meteor. Soc.,* **79,** 443–455.

Protat, A., J. Delanoë, A. Plana-Fattori, P. T. May, and E. J. O'Connor, 2010: The statistical properties of tropical ice clouds generated by the West African and Australian monsoons, from ground-based radar–lidar observations. *Quart. J. Roy. Meteor. Soc.,* **136,** 345–363, doi:10.1002/qj.490.

Rémillard, J., P. Kollias, E. Luke, and R. Wood, 2012: Marine boundary layer cloud observations at the Azores. *J. Climate,* **25,** 7381–7398.

Shupe, M. D., V. P. Walden, E. Eloranta, T. Uttal, J. R. Campbell, S. M. Starkweather, and M. Shiobara, 2011: Clouds at Arctic atmospheric observatories. Part I: Occurrence and macrophysical properties. *J. Appl. Meteor. Climatol.,* **50,** 626–644.

Stokes, G. M., and S. E. Schwartz, 1994: The Atmospheric Radiation Measurement (ARM) Program: Programmatic background and design of the cloud and radiation testbed. *Bull. Amer. Meteor. Soc.,* **75,** 1201–1221.

Tridon, F., A. Battaglia, and P. Kollias, 2013a: Disentangling Mie and attenuation effects in rain using a K_a-W dual-wavelength Doppler spectral ratio technique. *Geophys. Res. Lett.,* **40,** 5548–5552, doi:10.1002/2013GL057454.

——, ——, ——, E. Luke, and C. Williams, 2013b: Signal postprocessing and reflectivity calibration of the Atmospheric Radiation Measurements Program 915-MHz wind profilers. *J. Atmos. Oceanic Technol.,* **30,** 1038–1054.

Widener, K., and J. Mead, 2004: W-band ARM cloud radar—Specifications and design. *Proc. 14th ARM Science Team Meeting,* Albuquerque, New Mexico, ARM, 6 pp. [Available online at http://www.arm.gov/publications/proceedings/conf14/extended_abs/widener2-kb.pdf.]

Zink, M., E. Lyons, D. Westbrook, D. Pepyne, B. Pilips, J. Kurose, and V. Chandrasekar, 2008: Meteorological command and control: Architecture and performance evaluation. *2008 IEEE International Geoscience and Remote Sensing Symposium: Proceedings,* Vol. 5, IEEE, V-152–V-155, doi:10.1109/IGARSS.2008.4780050.